

Investigating the effect of using three pozzolans separately and in combination on the properties of self-compacting concrete

Milad Orak^{1a} and Fathollah Sajedi*¹

¹Department of Civil Engineering, Ahvaz Branch, Islamic Azad University, Ahvaz, Iran

(Received February 12, 2021, Revised May 18, 2021, Accepted May 22, 2021)

Abstract. Today, the tendency to use self-compacting concrete (SCC) is expanding because of its significant benefits. In this study, SCC was made by using native materials and then different pozzolans were replaced instead of a part of cement and the rheological and mechanical properties and microstructure of the concrete were investigated. The pozzolans containing of metakaolin (15%, 25% and 35%), silica fume (6%, 12% and 18%) and fly ash (20%, 35% and 50%) were replaced instead of a part of cement separately or simultaneously. Self-compaction tests including slump flow, T500, L-box, U-box, and J-ring as well as mechanical tests including compressive strength, splitting tensile strength, and static modulus of elasticity were performed on the specimens. The results showed that the pozzolans improved the microstructure of the SCC and the secondary reactions improved the mechanical properties of the concrete containing the pozzolans at older ages than the reference concrete. At 15% replacement, metakaolin increased the 180-day compressive strength up to 106 MPa that was about 18% more than reference concrete. In ternary mixtures the maximum and minimum rate were 29% and 19%, respectively, and in quaternary mixtures the rates were significant and increased up to 46%, while the rate for reference concrete was 20%. This significant growth was probably due to the secondary reaction of pozzolans with calcium hydroxide residue from cement hydration.

Keywords: fly ash (FA); limestone powder (LP); metakaolin (MK); microstructure; self-compacting concrete (SCC) properties; silica fume (SF)

1. Introduction

Concrete is one of the structural materials and nowadays it is difficult to find a construction project without using concrete (Zhang *et al.* 2019, Abedini and Zhang 2020, Sun *et al.* 2020, Xu *et al.* 2020b). Many researchers have studied the performance of concrete structures subjected to different loading conditions such as seismic loads (Zhu *et al.* 2018, Zhang and Wang 2019a, Alam *et al.* 2020a, c). In the last two decades, concrete is no longer a material made solely of cement, aggregate and water, but is an engineered material with new components and meets many of the amazing needs of the construction industry (Badry 2015, Alam *et al.* 2020b, Zhang *et al.* 2020b, Abedini and Zhang 2021). Advances in concrete technology have resulted in the development of a new type of concrete called self-compacting concrete (SCC) (Toghroli *et al.* 2017, Nosrati *et al.* 2018, Ziaei-Nia *et al.* 2018, Sun *et al.* 2019, Yazdani *et al.* 2020). The main feature of this type of concrete is based on two aspects of self-compacting and its high performance. SCC is an innovative concrete that does not need vibration for placing and compaction. Self-Compacting Concrete (SCC) is popular because it is a workable concrete with a

satisfactory level of strength (Memon *et al.* 2020, Shariati *et al.* 2020b). This concrete is able to fully fill the mold and achieve full compaction due to its weight being poured even in the presence of compacted reinforcements. Its hardened concrete is dense and homogeneous and has engineering properties and durability similar to that of normal vibrating concrete (NVC) (AK *et al.* 2018, Li *et al.* 2019, Yang *et al.* 2020).

Following the definition of EN 206: 2000, which has been updated to EN 206: 2013 + A1 2016, the concrete performance is determined not only by its mechanical properties but also by its rheological properties. Improvement of durability can be achieved significantly by the presence of supplementary cementitious materials (SCM) in the mixture (Badogiannis *et al.* 2015, Wang *et al.* 2020, Zheng *et al.* 2020, Wang *et al.* 2021). Due to the high pozzolanic activity and filling ability, SCM can produce a more durable, cohesive, and compacted concrete that will promote mechanical properties and reduce permeability (Güneyisi *et al.* 2008, Cassagnabère *et al.* 2010, Sfikas *et al.* 2014, Xu *et al.* 2020a).

SCC contains more fillers and admixtures than NVC, and its particle density is more uniform; therefore, the required viscosity and rheology will be provided. To achieve self-compaction properties, it is necessary to limit the volume of coarse materials, reduce the ratio of water to cement and using more superplasticizers (SP) (Madandoust *et al.* 2012, Yang *et al.* 2015, Toghroli *et al.* 2018, Afshar *et al.* 2020, Shariati *et al.* 2020c). It has been shown that modification of concrete with fine particles improves the

*Corresponding author, Associate Professor,
E-mail: sajedi@iauhvaz.ac.ir

^a Ph.D. Student,
E-mail: miladorak@gmail.com

Table 1 Limitations of fly ash types (C, F & N)

%	C	F	N
Minimum sum of silica, alumina and iron oxide	50	70	70
Maximum sulfur trioxide	5	5	4
Maximum moisture content	3	3	3
Maximum amount of thermal mass loss	6	6	10

mechanical properties and durability of concrete (Niewiadomki 2018). Active fillers have a positive effect on the delay in the process of concrete degradation and increase the toughness of the cementitious compounds (Zhang and Ou 2008, Golewski and Sadowski 2014, Golewski and Sadowski 2017, Abedini *et al.* 2020).

In this study, some rheological and mechanical properties of SCC have been investigated. In order to provide a scientific solution to protect the environment and move towards sustainable development, part of the cement has been replaced with different SEMs. For this purpose, Metakaolin (MK), Silica Fume (SF) and Fly Ash (FA) were replaced instead of cement separately with different percentages. Each of these SCMs was used in separate, binary, ternary and quaternary mixes.

1.1 Supplementary cementitious materials (SCMs)

SCMs are natural materials or industrial by-products that exhibit cementitious behavior when used with water and cement. In addition, alternative cementitious materials make the concrete mix extremely economical, improve strength, and reduce concrete permeability (Shariati *et al.* 2020a, Zhao *et al.* 2020, Zuo *et al.* 2020, Zhang *et al.* 2021).

The SCMs react with calcium hydroxide, which is released through the cement hydration, and is converted to Calcium Silicate Hydrate (C-S-H). This is called the pozzolanic reaction. As pozzolan reacts with calcium hydroxide and consumes it, which is a poor component of cement paste and improves concrete microstructure, it increases the durability of concrete against destructive factors (Shariati *et al.* 2019a, Trung *et al.* 2019, Toghroli *et al.* 2020, Mehrabi *et al.* 2021, Rajaei *et al.* 2021). The pozzolanic reaction rate is generally slow and consequently the heating rate will be slow which makes these products usually a good choice for mass concrete (Memon *et al.* 2018, Liu *et al.* 2020b, Zhang *et al.* 2020c). Mechanical properties were of SCC affected by the cementitious materials used. The effect is significant on certain types of pozzolans such as silica fume and fly ash (Behfarnia and Hasanzade 2014, Zhang *et al.* 2019, Liu *et al.* 2020a, Xu *et al.* 2021).

ASTM C618 has defined the FA and natural pozzolans that shall conform to the requirement as to chemical composition prescribed in Table 1.

MK is a white amorphous (non-crystalline) silicate that has pozzolanic properties and is classified as N class Pozzolans by ASTM C618. It is obtained by calcination of the kaolinite clay at 500 to 800°C. Due to the highly irregular texture of MK, it reacts rapidly with calcium hydroxide generated by the hydration action and produces

calcium silicate hydrate gel. (Hassan *et al.* 2010) investigated the effect of MK on SCC rheology and found that by increasing the amount of MK in SCC mixtures from 0 to 27%, the demand for SP increased to 25%. (Vejmelková *et al.* 2011) investigated the effect of MK and slag on the properties of SCC and reported that adding MK to SCC increased the amount of water needed and this concrete lose its rheology relatively quickly over time. This is attributable to the higher side surface area of cement gel with MK due to its high reactivity rate, which is why the compressive strength (CS) of the SCC containing MK grows very rapidly during the initial hardening period. Gruber *et al.* (2001) evaluated the durability of the concrete containing MK and concluded that MK with high reactivity reduces permeability of chloride in concrete and extremely effects on life of reinforced concrete in environment containing chloride. Badogiannis and Tsivilis (2009) investigated the effect of MK on the durability of concrete and concluded that the addition of MK caused a relative decrease in the adsorption of the concrete. Poon *et al.* (2003) examined the pozzolanic reaction temperature of high performance cement paste mixed with MK and compared it with cement paste mixed with SF and FA. It was reported that the pozzolanic rate of MK was higher than that of SF and decreased with increasing age, reaction rate is reduced for both MK and SF, but this decrease was greater for MK.

SF is a by-product of the melting process in the ferrosilicon manufacturing industry. It is usually a gray powder somewhat similar to ordinary Portland cement or FA and can have both pozzolanic and cementitious properties (Zhang *et al.* 2006, Siddique and Khan 2011, Zuo *et al.* 2015, 2017). by replacing SF and MK pozzolans separately and simultaneously, it has been concluded that these pozzolans increase water demand in fresh concrete and decreases the short-term strength of concrete, while also increases its long-term strength. Also, researchers found that the engineering properties of SCC are improved by replacing different percentages of SF.

FA is also known as burnt ash, is produced through burning of soft coal by electric power of electricity plant. The size of FA particles depends on the type of equipment used for collecting dusts and is usually smaller than ordinary Portland cement with a diameter in the range of 1 to 150 μm (Sun *et al.* 2018, Zhang and Wang 2019b, Shariati *et al.* 2020d). Jalal *et al.* (2015) tried to explore its properties by replacing a part of cement with FA and SF in self-compacting reinforced concrete. They found that the FA improved the concrete rheology, while SF improved the mechanical properties of the concrete.

2. Laboratory program

2.1 Characteristics of used materials in research

In this study, ordinary Portland cement type 2 produced by Khouzesan Cement Company with the specific surface of 2.561 g/cm^3 has been used to construct mixtures of SCC. High fineness limestone powder (passing through sieve No. 140) and apparent specific weight of 2.561 g/cm^3 were also

Table 2 Chemical composition of limestone powder (LP) and cementitious materials used in the research

Materials Used	%	Al ₂ O ₃	CaO	Na ₂ O	K ₂ O	SiO ₂	SO ₃	Fe ₂ O ₃	MgO	LOI
Cement	-	4.60	63.44	0.24	0.79	21	2.56	3.54	2.42	1.36
MK	0.45	15.69	1.46	0.01	0.04	80.76	0.12	0.04	0.05	--
SF	--	0.41	3.15	0.01	0.10	94.68	0.12	--	0.09	--
FA	--	18.08	39.35	0.05	0.11	38.28	--	3.06	0.21	3.007
LP	1.24	4.05	10.05	0.25	0.023	15.47	0.5	2.3	17.63	42.13

Table 3 Physical characteristics of the stone materials used in the research

Type of stone materials	Maximum size (mm)	Specific weight (g/cm ³)	Water absorption (%)	Available humidity (%)
Sand	5	2.65	0.6	0
Fine aggregate	9.5	2.56	1	0
Coarse aggregate	19.5	2.63	0.8	0

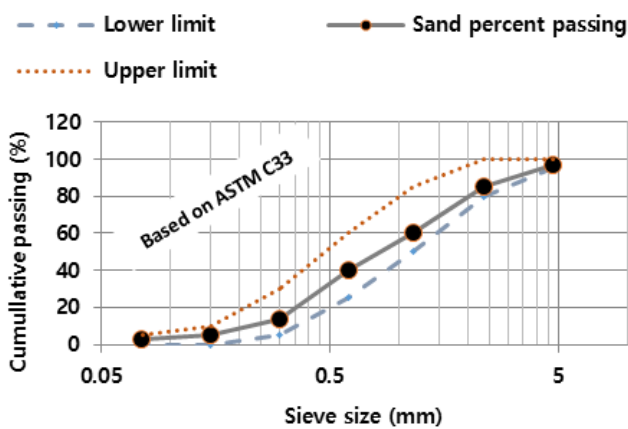


Fig. 1 Grading curve of the sand used in the study

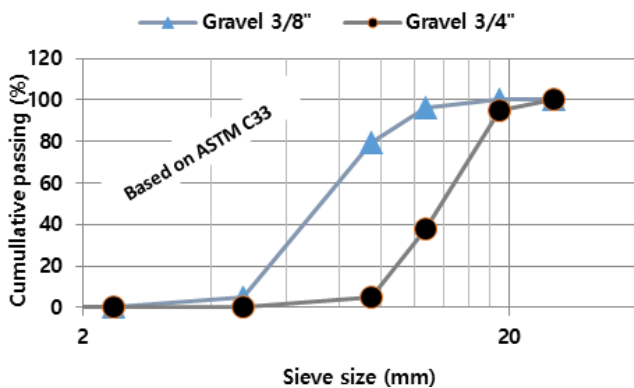


Fig. 2 Grading curves of the gravel used in the study

used as viscosity modifying agent (VMA). The pozzolanic materials used in the study are MK, SF, and FA with an average particle size of 37 μm (equivalent to 400 mesh) and are manufactured by the Jahan Powder Group, Delijan, Iran. The chemical compositions of cement, limestone powder and pozzolanic materials used in the study were determined using X-ray fluorescence spectroscopy and have been presented in Table 2.

In order to prepare the desired mixture, twice washed broken sand in two different sizes were used. The physical Andimeshk river sand with fineness modulus of 4.8 and

properties of the stone materials used in the research have been presented in Table 3 and their grading curves have been shown in Figs. 1 and 2. SP based on brown polycarboxylate ether with a specific weight of 1.07 g/cm^3 produced by Fabir Company were also used to provide the required flow ability.

2.2 Details of the research mix design

In this study, the construction and test of 20 concrete mixtures (including a reference SCC (Ctrl) and 19 SCC mixtures containing pozzolans with different replacement percentages as binary, ternary, and quaternary mixtures) were studied. The details of the research mix design have been given in Table 4. In SCC mixtures, the Ctrl was first made to reach the requirements for rheology, then in the other mixtures, pozzolans of the MK, SF, and FA with different percentages (binary, ternary and quaternary) were replaced some parts of the cement. In all made mixtures, the amount of sand, fine aggregate, coarse aggregate, limestone powder and water to binder ratio were kept constant. Levels of polycarboxylate SP were determined for all mixtures visually by gradual addition to achieve the required flow ability.

2.3 Casting mixtures

Rotary mixers with fixed blades and 300-liter capacity were used to make the concrete mixtures and the mixing procedure was applied for all mixtures through similar process. First, the aggregates (all sand and gravel) were poured dry in the static mixture, then 10% of mixing water was added to them and stirred for 30 seconds, then was stopped three minutes. Next, the mixer was started and the limestone powder was slowly added, then the pozzolan mixed with 50% of the mixing water was gradually added. 30 seconds later, the cement and immediately SP combined with the residual water were added to the mixture. Finally, the SCC was mixed for another 2 minutes. The mixtures were made at an average temperature of 32°C and relative humidity of 50%. It is noteworthy that the order and percentage of addition of materials to the concrete mix was based on the researcher's experience.

Table 4 Research mix design details

Mix No.	Mix design	C	W	S	FAG	CAG	LP	SP	MK	SF	FA
1	Ctrl	546.4	218.6	948.4	233.4	311.2	105.1	8.197	-	-	-
2	MK15	464.4	218.6	948.4	233.4	311.2	105.1	8.197	82	-	-
3	MK25	409.8	218.6	948.4	233.4	311.2	105.1	7.650	136.6	-	-
4	MK35	355.2	218.6	948.4	233.4	311.2	105.1	6.010	191.2	-	-
5	SF6	513.7	218.6	948.4	233.4	311.2	105.1	8.197	-	32.8	-
6	SF12	408.8	218.6	948.4	233.4	311.2	105.1	8.197	-	65.6	-
7	SF18	448.1	218.6	948.4	233.4	311.2	105.1	6.556	-	98.4	-
8	FA20	437.1	218.6	948.4	233.4	311.2	105.1	8.197	-	-	109.3
9	FA35	355.2	218.6	948.4	233.4	311.2	105.1	6.830	-	-	191.2
10	FA50	273.2	218.6	948.4	233.4	311.2	105.1	5.846	-	-	273.2
11	MK15 SF12	398.9	218.6	948.4	233.4	311.2	105.1	7.103	82	65.6	-
12	MK25 SF12	344.3	218.6	948.4	233.4	311.2	105.1	7.923	136.6	65.6	-
13	MK15 FA20	355.2	218.6	948.4	233.4	311.2	105.1	6.721	82	-	109.3
14	MK25 FA20	300.1	218.6	948.4	233.4	311.2	105.1	6.770	136.6	-	109.3
15	SF12 FA20	371.5	218.6	948.4	233.4	311.2	105.1	6.556	-	65.6	109.3
16	SF12 FA35	289.6	218.6	948.4	233.4	311.2	105.1	6.556	-	65.6	191.2
17	MK15 SF6 FA35	240.6	218.6	948.4	233.4	311.2	105.1	6.666	82	32.8	191.2
18	MK25 SF6 FA35	185.8	218.6	948.4	233.4	311.2	105.1	6.104	136.6	32.8	191.2
19	MK15 SF12 FA35	207.6	218.6	948.4	233.4	311.2	105.1	1.101	82	65.6	191.2
20	MK25 SF12 FA20	234.9	218.6	948.4	233.4	311.2	105.1	6.720	136.6	65.6	109.3

Notice: Water to binder ratio was constant as 0.4 for all the mixtures

Table 5 Allowed range values for fresh self-compacting concrete (The European Guidelines for SCC 2005)

Test	Property	Max.	Min.	Unit
Slump flow	Filling ability	800	650	mm
J-ring	Passing ability	10	0	mm
L-box	Passing ability	1	0.8	-
U-box	Flow ability	30	0	mm

2.3.1 Fresh concrete tests

Five different tests were performed for each mixture related to the rheological behavior of fresh concrete (Shariati *et al.* 2019b). Performance was tested using slump flow test according to ASTM C1611, T500 test, passing ability was tested with L-box and J-ring tests according to EN 12350 and ASTM C1621 and flow ability was evaluated with U-box test according to EN 11044. The mixtures were classified in terms of rheology according to the European Guidelines for SCC (2005). This guideline defines the permissible ranges for the various SCC tests that have been presented in Table 5.

2.3.2 Hardened concrete tests

For each mixture, 12 cubic specimens with 100×100×100 mm dimensions and 7 standard cylindrical specimens were casted. A total of 380 different specimens were prepared for the purpose of this study. The specimens were kept in the molds for 24 hours in the laboratory and then the molds were opened and the specimens were stored in a

20±2°C water tank and they were treated in accordance with EN 12390. At the age required for the test, the specimens were removed from the reservoir one hour before the start of the test and kept in a laboratory environment without any excess moisture.

At the end of the treatment period, the specimens were tested according to the related standards. CS was carried out on cubic specimens at 7, 28, 91 and 180 days of age, and splitting tensile strength (SPT) at 28 days of age and static modulus of elasticity at 28 and 91 days of age were performed on standard cylindrical specimens. Scanning electron microscope (SEM) images at 28 days of age were taken to investigate the microstructure of pozzolanic SCC.

3. Analysis of experimental results

3.1 Fresh concrete tests

In this study, to evaluate the self-compacting properties of concrete, five experiments of slump flow, T500, L-box, U-box and J-ring were carried out on fresh concrete based on the European Guideline for SCC (2005). Pictures of self-compacting tests have been shown in Fig. 3. The results of the self-compaction tests have been presented in Table 6.

3.1.1 Slump flow test

This test was performed according to ASTM C1611 to evaluate the flow and filling ability of fresh SCC with a maximum aggregate size of 25 mm. The permissible range recommended by the European Guidelines for SCC (2005)

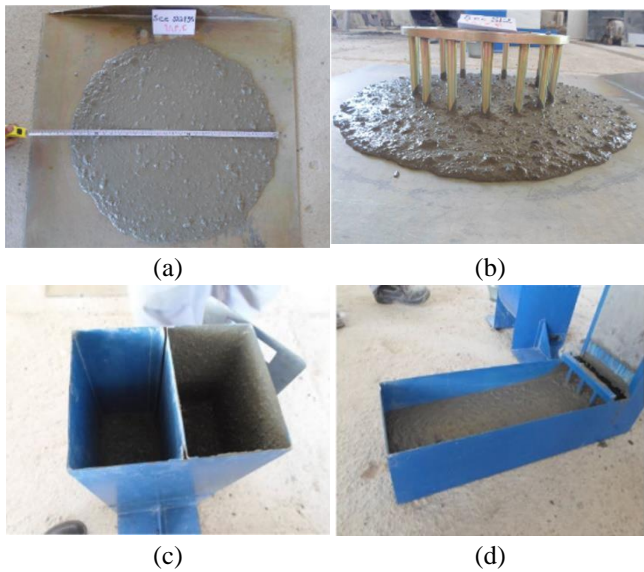


Fig. 3 SCC tests performed

Table 6 Results of self- compacting concrete tests in fresh state

Mix no.	Mix design	Slump flow (mm)	T ₅₀₀ (sec)	U-Box (mm)	J-Ring (mm)	L-Box
1	Ctrl	695	1.5	8	665	0.91
2	MK15	640	1.8	10	610	0.88
3	MK25	650	2	5	620	0.88
4	MK35	800	1.25	5	770	0.94
5	SF6	810	1.5	6	580	0.85
6	SF12	660	1.8	20	630	0.76
7	SF18	630	2	21	600	0.875
8	FA20	775	1.5	5	745	0.95
9	FA35	720	1.5	5	690	0.89
10	FA50	710	1.5	10	680	0.94
11	MK15 SF12	645	1.8	11	615	0.89
12	MK25 SF12	815	1.5	1	785	0.98
13	MK15 FA20	760	1.5	5	730	0.91
14	MK25 FA20	695	2	13	665	0.94
15	SF12 FA20	700	1.5	7	670	0.96
16	SF12 FA35	700	1.8	10	670	0.91
17	MK15 SF6 FA35	760	1.5	2	730	0.96
18	MK25 SF6 FA35	645	1.8	9	615	0.9
19	MK15 SF12 FA35	630	1.8	5	600	0.86
20	MK25 SF12 FA20	675	1.8	10	645	0.87

for the results of this experiment is 650 to 800 mm. According to the results presented in Table 6, the slump flow value of the reference SCC was 695 mm, which is within the permissible range. By applying a portion of cement with SCM, the slump flow was in the range of 610 to 815 mm, which was within the permissible range or their distance to the permissible range was very low.

3.1.2 T500 test

The T500 test has been proposed by the European Guide of SCC (2005) as an optional test in conjunction with slump flow test to determine the flow rate and relative viscosity of SCC mixtures. The T500 reaches the outer edge of the concrete circle with a flow diameter of 500 mm, which is measured by a timer during slump flow testing. The permissible range recommended by the European Guidelines for SCC (2005) is 2 to 5 seconds. The results for the T500 test were in the range of 1.25 to 2 seconds, indicating the very low relative viscosity and internal stress of SCC mixtures.

3.1.3 U-box test

The method of conducting this test according to EN 11044 is presented for evaluation of the flow ability of SCC. In this experiment, the height difference of the concrete in the two chambers is considered as the number of the U-box test. The European Guideline for SCC (2005) has been recommended a maximum of 30 mm for this experiment. The results presented in Table 6 show that all the numbers obtained from the different SCC mixtures were in the range of 1 to 21 mm, indicating their very good flow ability.

3.1.4 J-ring test

The method of performing this test according to ASTM C1621 is presented to evaluate the fresh SCC in terms of passing ability. According to the results presented in Table 6, the values obtained for the J-ring in all mixtures were in the range of 580 to 785 mm, which were within the permissible range, indicating the appropriate passing ability of these mixtures in the face of obstacles.

3.1.5 L-box test

The method of conducting this test according to EN 12350 is presented to evaluate the passing ability and filling ability of fresh SCC and to examine the possibility of SCC blocking in the face of reinforcement. For this purpose, the concrete height reduction is measured at the beginning of the horizontal part of the box (H1) and at the end of the horizontal part of the box (H2). The number of L-boxes is obtained by dividing H2 to H1. This number must be in the range of 0.8 to 1 according to EN 12350. The results presented in Table 6 show that all the numbers obtained from the various SCC mixtures were within the permissible range except the SF12 mix design whose difference was negligible.

3.2 Hardened concrete tests

3.2.1 Compressive strength

The effect of different pozzolans at 7, 28, 91 and 180 days on CS of SCC presented in Table 7 and has been shown in Fig. 4. As expected, the CS of all mixtures increased with age. At 7 days of age, the CS of all mixtures containing pozzolan was lower than the Ctrl. Meanwhile, SF had the least strength and MK had the highest strength. At 28 days of age, the SCC containing of MK had a higher rate of growth strength than the other two pozzolans. At this

Table 7 Compressive strength test results at different ages (MPa)

Mix no.	Mix design	7 days		28 days		91 days		180 days		Rate change compared to Ctrl at 28 days (%)
		CS	SD	CS	SD	CS	SD	CS	SD	
1	Ctrl	65.1	3.25	75.3	2.15	79.6	3.46	90.2	4.21	19.7
2	MK15	61.3	2.63	79.7	3.26	91.6	4.27	106.0	2.30	40.8
3	MK25	56.3	2.21	72.6	2.93	84.6	3.87	89.1	3.15	18.4
4	MK35	52.4	3.60	65.5	3.25	70.7	5.12	72.3	2.39	-4.0
5	SF6	58.7	4.20	76.4	3.86	80.1	4.89	92.2	4.96	22.5
6	SF12	62.8	4.15	78.9	4.72	84.6	4.29	89.8	3.24	19.2
7	SF18	55.6	5.32	72.3	3.99	76.0	2.81	80.4	5.86	6.8
8	FA20	57.6	2.85	72.0	2.96	79.8	3.69	87.2	3.71	15.8
9	FA35	51.8	2.23	69.7	1.85	74.3	2.18	79.2	2.36	5.1
10	FA50	42.1	3.56	59.4	2.13	63.7	4.32	69.0	3.16	-8.4
11	MK15 SF12	51.4	1.78	56.1	2.36	66.7	4.28	72.0	3.02	-4.4
12	MK25 SF12	51.9	4.65	62.0	3.12	68.7	6.01	77.2	3.23	2.5
13	MK15 FA20	51.3	3.12	58.2	3.25	65.7	2.63	69.3	5.68	-8.0
14	MK25 FA20	37.7	2.56	54.3	3.46	61.8	2.36	66.5	2.35	-11.7
15	SF12 FA20	56.4	3.25	61.5	2.18	65.4	1.45	79.4	2.22	5.4
16	SF12 FA35	39.1	1.98	54.9	2.56	56.4	2.17	69.9	3.12	-7.2
17	MK15 SF6 FA35	28.5	3.62	46.3	3.03	62.2	2.69	67.6	2.15	-10.2
18	MK25 SF6 FA35	29.3	4.02	43.1	2.72	53.5	3.12	54.7	2.48	-27.3
19	MK15 SF12 FA35	28.5	3.51	42.1	4.83	46.4	2.84	50.9	3.56	-32.4
20	MK25 SF12 FA20	33.3	3.29	42.0	4.11	53.3	2.45	57.7	3.11	-23.3

CS: compressive strength; SD: standard deviation

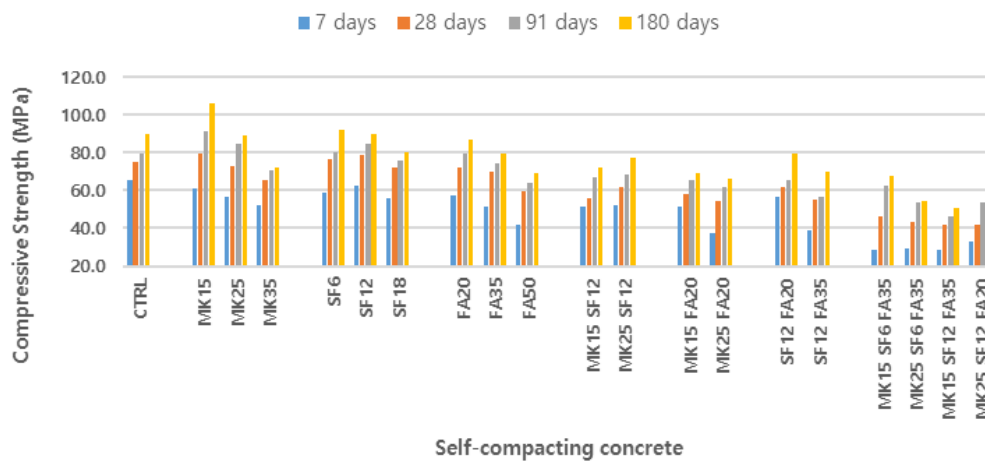


Fig. 4 Compressive strength of SCC mixtures in different ages

age, by replacing part of the cement with MK and SF, more CS was obtained than the Ctrl at the same age, whereas FA replacement showed less CS than the Ctrl. Fernandez *et al.* reported in a similar study the improvement of CS or reported that replacement of cement with MK at 7 days of age resulted in improved CS. However, (Marsh and Day 1988) reported a negligible contribution of FA in strength until about 14 days of age.

The results of the 91-day experiments also showed a good CS growth rate for all mixtures at all replacement

levels. Replacement of 15% MK increased about 15% of CS at 91 days of age compared to the Ctrl at the same age, which could be explained by the improvement of the concrete microstructure by performing secondary MK reactions. (Khodabakhshian *et al.* 2018) reported the replacement of 10% SF significantly increases the CS compared to the Ctrl.

It can be seen in Fig. 4 that all ternary and quaternary mixtures had less CS than all binary mixtures at all ages. It is important to note that the growth rate of strength

increases with age, especially in quaternary mixtures, and considering the high replacement levels (56% to 66%), the considerable CSs has been achieved. It is also evident that with increasing percentages of replacement of MK and FA, the CS of all ages decreased at almost constant rates.

The results of CS at the age of 180 days showed a growth for all mixtures compared to the results of 91 days of age. The highest CS was for the SCC containing of 15% MK that showed 106 MPa at the age of 180 days, while it was 33% more than the result of 28 days of the same mixture and 16% more than the results of the Ctrl at the same age.

Studies have indicated that the performance of pozzolanic SCC was better than that of ordinary pozzolanic concrete because it had on average about 7% more compressive strength. It was reported the rapid pozzolanic activity of SF and the conversion of calcium hydroxide crystals to gels as well as their filling properties result in greater strength of SCC than NVC. In the present study, these effects have been observed not only in the replacement of MK but also in FA. It should be noted that these effects were especially higher for binary and ternary mixtures and the percentage of increase in CS with increasing age of the specimens for these mixtures was higher than the Ctrl or binary mixtures. (Guo, Jiang *et al.* 2020) also found that as the age increased, the percentage of increased CS due to binary and ternary mixtures (FA, SF and slag) was higher than the Ctrl without pozzolan or binary mixtures. (Ardalan *et al.* 2017) observed that as a result of single replacement of FA and pumice, the CS of the Ctrl decreased but the CS could be increased through binary mixtures with SF. The last column of Table 7 presented the increase in long-term (180 days of age) CS compared to standard (28 days of age) CS in SCC mixtures.

The study of the process of achieving CS shows that the amount of long-term CS in quaternary mixtures compared to ternary and binary mixtures has increased by 81% and 31%, respectively, and ternary mixtures have increased by 39% more than binary mixtures. Therefore, in comparison between the use of pozzolans in binary, ternary and quaternary mixtures in the process of achieving CS by age, compared to the Ctrl at the age of 28 days, quaternary mixtures to binary and ternary mixtures is strongly recommended. But, when CS results in 180 days of age compared to Ctrl in 28 days of age, observed that binary mixtures on average gained 13% higher CS than the reference mixture at 28 days of age, while the average CS achieved for ternary and quaternary mixtures at 180 days of age was 4% and 23% less, respectively, in compared to the CS of the reference mixture at 28 days of age. Therefore, in comparison between the effect of pozzolans in binary, ternary and quaternary mixtures, compared to Ctrl at the age of 28 days, binary mixtures are really preferred to ternary and quaternary.

Due to the secondary reaction of the pozzolans, the long-term compressive strength of mixtures containing alternative SCMs has improved and the growth rate has increased with increasing replacement rate. However, the decrease in compressive strength compared to the Ctrl at the age of 28 days in ternary and quaternary mixtures was due to the decrease in the amount of cement used. This cannot

be considered a negative factor because in the mixture containing the highest amount of replacement (66% in the MK25 SF6 FA35 mixture) the compressive strength decreased by only 27%, which indicates the effectiveness of the pozzolans.

3.2.2 Splitting tensile strength

Tensile strength in SCC is of particular importance. The results of splitting tensile strength test (SPT) presented in Table 8 and has been shown in Fig. 5. Application of MK resulted in improved SPT compared to the Ctrl. At 15% replacement, the SPT increased by 10% compared to the Ctrl but the growth rate decreased as the replacement percentage increased, so that by 35% replacement, the SPT decreased compared to the Ctrl. With the increase in the percentage of SF replacement, the SPT of SCC was initially increased to about 6%, but at 18% replacement, this strength decreased to 15% compared to the Ctrl. All percentages of FA replacement decreased the SPT and with increasing the amount of replacement, the strength loss was also increased. (Iris, Belen *et al.* 2017) reported the behavior of SCC in SPT similar to that of NVC. stated that the SPT of concrete has a behavior similar to that of CS and increases with time, but its increase trend slows down over time compared to the CS. This is also seen in the results of the present study.

As shown in Fig. 6, it is evident that in all ternary and quaternary replacement, the SPT have significantly decreased compared to the Ctrl strength. However, the rate of strength loss in quaternary mixtures was higher than that of ternary mixtures. The maximum strength loss was related to the MK15 SF12 FA35 quaternary mixtures that its SPT was decreased by about 48%, and the lowest strength loss was related to the SF12 FA20 ternary mixtures with SPT loss of about 28%. It is important to note that in the quaternary mixture, the cement used was 62% lower than the cement used in Ctrl.

Fig. 6 illustrates the relationship between the SPT and the CS of made SCC at 28 days of age. It is observed that the process of achieving SPT with increasing age is proportional to the process of achieving CS but its increase/decrease rate is different from the increase/decrease rate of the compressive strength.

Guo *et al.* (2020) observed that binary or ternary mixtures reduced the SPT by 17.2% to 89%, while in quaternary mixtures, the SPT significantly increased by about 10.2% compared to the no-pozzolan mixture. This is also seen in the findings of this study.

By analyzing the results of SPT as presented in Table 8, observed that binary, ternary and quaternary mixtures on average gained 16%, 23% and 36% less SPT than Ctrl, respectively. It can be found that using of SCMs have not positive effect on SPT results and the SPT results decreased by increasing replacement level in comparison with Ctrl. This effect may be less due to the use of cement, and possibly at older ages, the pozzolanic reaction of SCMs will compensate for this difference.

3.2.3 Static modulus of elasticity

The SME of concrete is a crucial mechanical property in design and analysis of concrete structures, for example,

Table 8 Tensile strength (SPT) and static modulus of elasticity (SME)

Mix no.	Mix design	SPT				SME	
		28 days (MPa)	SD (MPa)	28 days (MPa)	SD (MPa)	28 days (MPa)	SD (MPa)
1	Ctrl	5.66	0.35	3.9	0.22	4.1	0.22
2	MK15	4.58	0.33	3.4	0.18	3.7	0.21
3	MK25	4.73	0.32	3.3	0.17	3.8	0.36
4	MK35	4.47	0.31	3.0	0.19	3.2	0.22
5	SF6	5.07	0.36	4.0	0.2	4.1	0.28
6	SF12	4.73	0.26	3.6	0.19	4.3	0.33
7	SF18	4.82	0.35	2.3	0.14	3.1	0.15
8	FA20	5.19	0.42	2.2	0.14	3.6	0.16
9	FA35	4.66	0.36	3.2	0.17	3.4	0.18
10	FA50	4.52	0.38	2.7	0.18	2.8	0.12
11	MK15 SF12	3.96	0.21	2.8	0.12	3.3	0.13
12	MK25 SF12	4.16	0.25	3.2	0.14	3.2	0.16
13	MK15 FA20	4.36	0.25	2.7	0.11	3.6	0.14
14	MK25 FA20	4.30	0.21	2.3	0.11	3.4	0.15
15	SF12 FA20	4.64	0.29	2.8	0.12	3.3	0.19
16	SF12 FA35	4.44	0.3	2.3	0.13	2.6	0.10
17	MK15 SF6 FA35	4.13	0.28	2.7	0.11	3.7	0.21
18	MK25 SF6 FA35	3.50	0.23	2.3	0.18	2.9	0.21
19	MK15 SF12 FA35	3.36	0.15	3.0	0.16	2.6	0.16
20	MK25 SF12 FA20	3.68	0.22	2.6	0.13	3.0	0.12

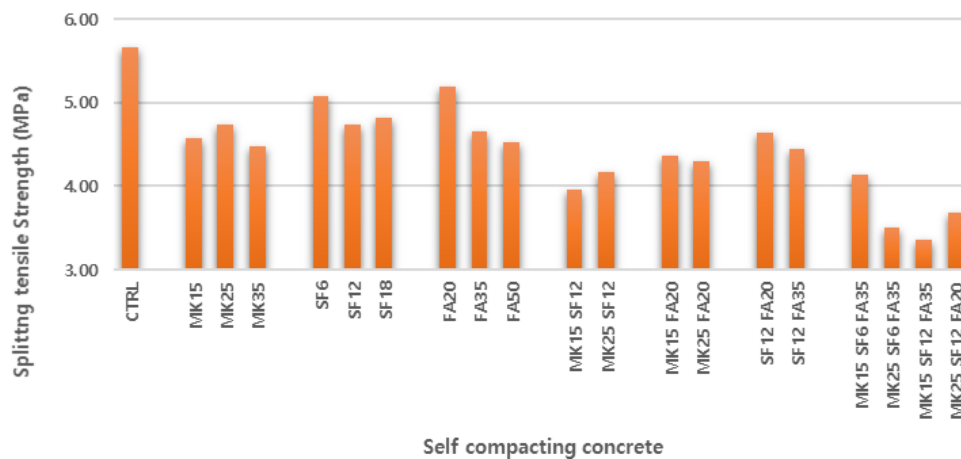


Fig. 5 The SPT results at 28 days of age of the specimens

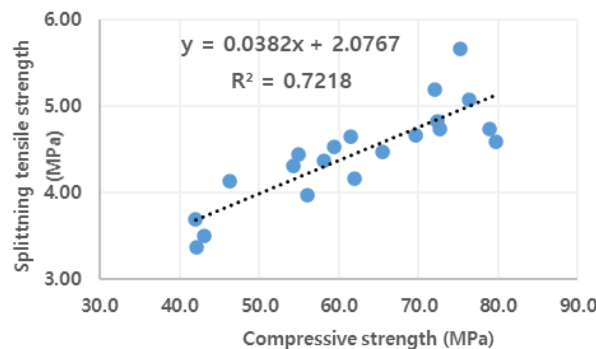


Fig. 6 Relationship between SPT and CS of specimens at 28 days of age



Fig. 7 SME test setup to determine static modulus of elasticity

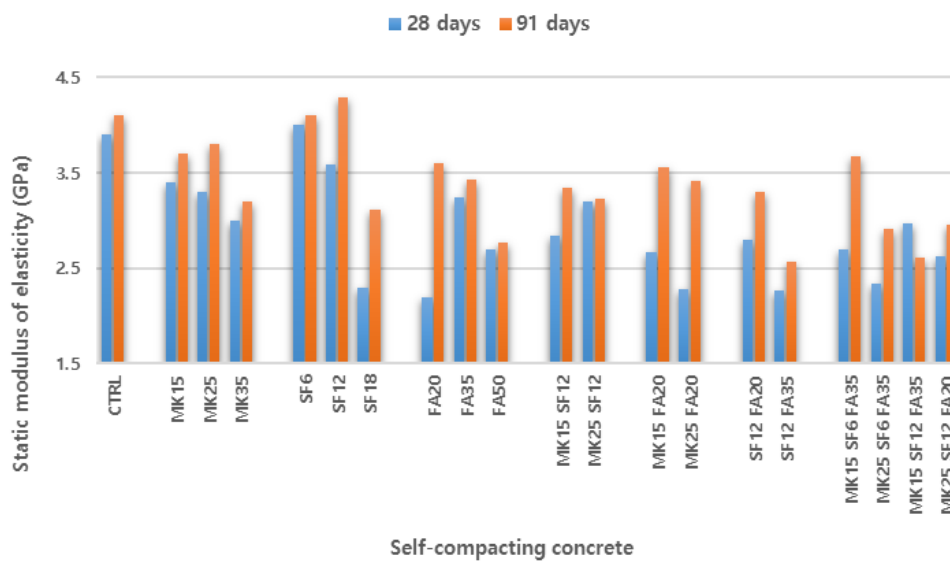


Fig. 8 Changes in the SME of the specimens at 28 and 91 days of age

member deflections for serviceability requirements, seismic analysis, drift calculations, elastic shortening of concrete in pre-stressed concrete design, and creep losses (Golafshani and Ashour 2016). The SME of SCC were applied on standard cylinders at 28 and 91 days of age, as described in ASTM C469. The SME test setup utilized in this research presented in Fig. 7. The results of the experiment are presented in Table 8 and have been shown in Fig. 8.

The concrete SME depends on the SME of the components and their percentage in the concrete volume. The SME of concrete is a function of its CS (ACI 1995). As can be seen in Fig. 6, the SME of all SCC mixtures containing pozzolans was lower than the Ctrl. The trend of improvement in SME has increased with age for concrete containing pozzolans, and this improvement has been further enhanced by increasing the amount of replacement of pozzolans. Fig. 9 shows the relationship between SME and CS of SCC made at 28 days of age. It can be seen that the trend of increasing the SME with increasing age is proportional with the trend of increasing the CS, but its growth rate is lower than the growth rate of compressive strength.

By comparing the results presented in second and third

columns of Table 8, it can be founded that results of SME as reference, binary, ternary and quaternary mixtures at 91 days of age, growth 5%, 16%, 21% and 11% compared to results at 28 days of age. So, it should be mentioned that ternary mixtures have the best performance in rate of growth by age. When the results of SME at 91 days of age compared to Ctrl at 28 days of age, observed that binary, ternary and quaternary mixtures on average gained 9%, 21% and 24% less SME than Ctrl, respectively. Therefore, it was concluded that SME results on average, decreased at all multiple pozzolanic mixtures, although, SF12 showed the best performance in SME at all ages.

Analysis of the results presented in Table 8 shows that the use of SCMs initially reduced the SME but with increasing age, had a good growth rate, which is probably due to the improvement of concrete microstructure as a result of pozzolanic reactions.

Fig. 10 shows the relationship between SME and CS of SCC made at 91 days of age. It is observed that the SME at 91 days also behaves similar to the SME at 28 days but its growth rate is different. The relationship between the SME at 28 days and 91 days has been shown in Fig. 12. According to Figs. 9 and 11, it can be concluded that the

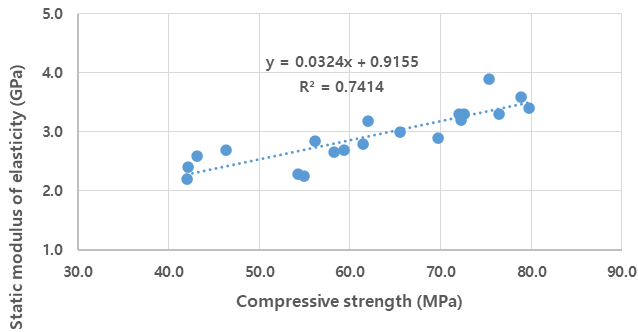


Fig. 9 Relationship between SME and CS of the specimens at 28 days of age

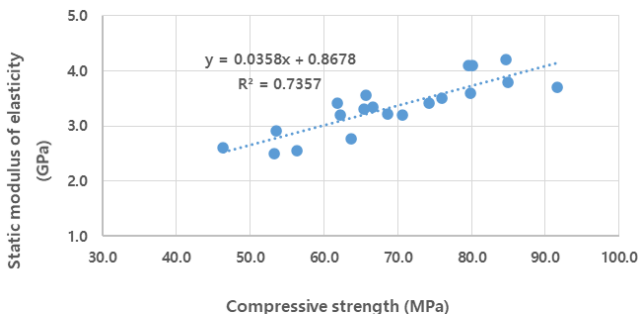


Fig. 10 Relationship between SME and CS of the specimens at 91 days of age

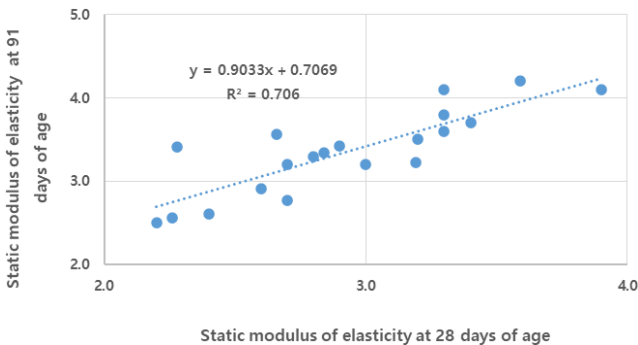


Fig. 11 Relationship between SME specimens at 28 and 91 days of age

SME of all specimens is improved with age, but their growth rate is different due to different pozzolanic behaviors.

3.3 Microstructural analysis of the specimens

Scanning Electron Microscopy (SEM) images were taken at 28 days of age to investigate changes in the microstructure of SCC due to the application of different pozzolans. In producing images, attention has been paid to the porosity, fine cracks, quality of ITZ between cement paste and aggregates, and the quality of hydration products. The SEM image of the reference SCC is shown in Fig. 12. The microstructure image of this concrete shows a heterogeneous texture with large needle-shaped calcium hydroxide crystals. In this Fig., large cavities have been seen along with small cracks.

SEM images of SCC by binary mixtures of the MK, SF,

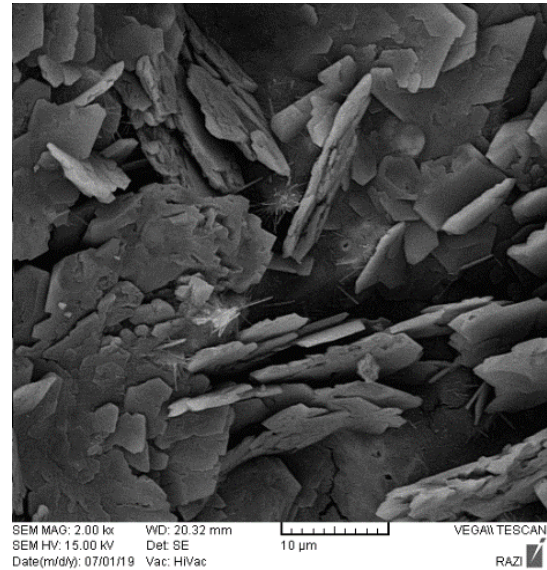


Fig. 12 SEM image of reference specimen

and FA pozzolans have been shown in Fig. 13. As can be seen in this Fig. 13, the microstructure of the concrete has been further deformed by using pozzolans and the size of the cavities has been reduced. The formation of hydrated calcium silicate gel (C-S-H) is evident from the reaction of calcium hydroxide with water and pozzolan in these images, which improves the properties of concrete and can lead to secondary reactions.

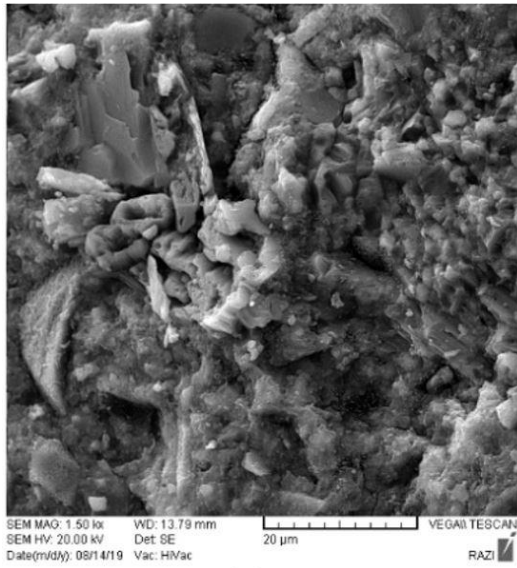
Fig. 13(a) shows the microstructure of the SCC containing MK in which the cavities became more regular than the Ctrl, while the size of the cracks was much finer and the presence of residual calcium hydroxide remaining from initial hydration is observed.

Fig. 13(b) shows the microstructure of SCC containing SF in which large crystals are transformed into small crystals and the amount of C-S-H increased. Small holes and cracks can also be seen in this image.

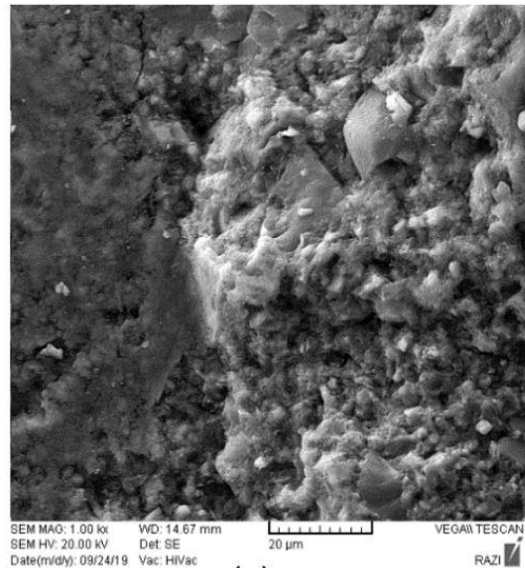
Fig. 13(c) shows that the reactivity of the FA resulted in a sharp decrease in the crystals but large cavities and cracks were observed that could decrease the CS of the concrete. This is also evident in the results of the CS test.

The microstructure of SCC with ternary mixtures has been shown in Fig. 14. In these mixtures, the concrete has a more amorphous structure and becomes more homogeneous and no calcium silicate gel or ettringite is observed in it. In these images, it is obvious that the size and volume of holes are reduced, but the poor quality of the ITZ between the cement paste and the aggregates is observed along with the large cracks.

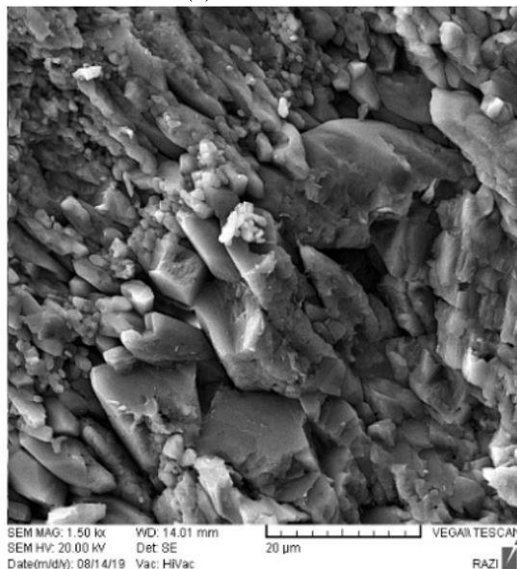
The microstructure of SCC with quaternary mixtures has been shown in Fig. 15. It is apparent in these images that the crystals have increased sharply as they have become smaller. In these mixtures, the homogeneity and density of the concrete were improved compared to the other mixtures, and the volume of the cavities decreased significantly. The quality of the ITZ is also better than the binary and ternary mixtures, but with increasing crystalline content, it is expected that the strength of these mixtures to be less than Ctrl or binary and ternary mixtures. In addition, due to the



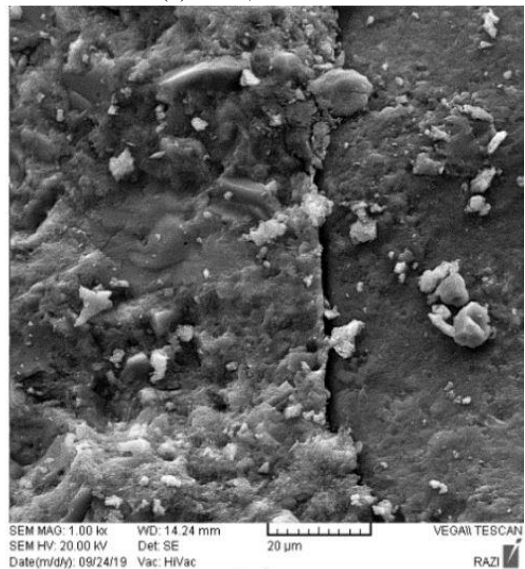
(a) OPC & FA



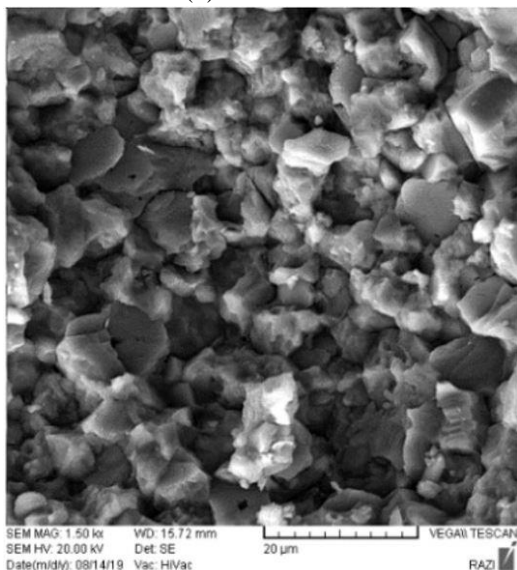
(a) OPC, MK & FA



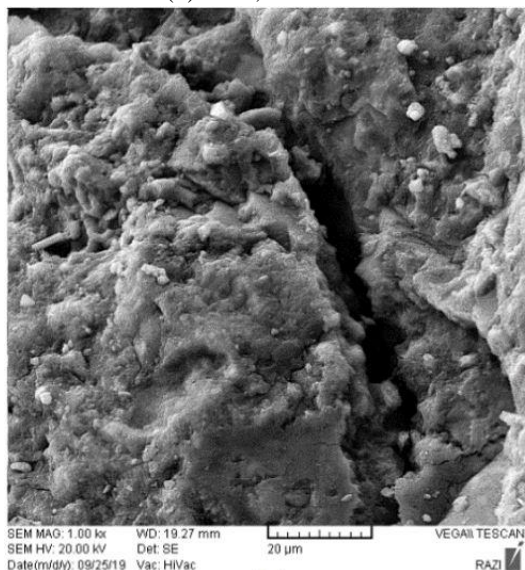
(b) OPC & SF



(b) OPC, SF & FA



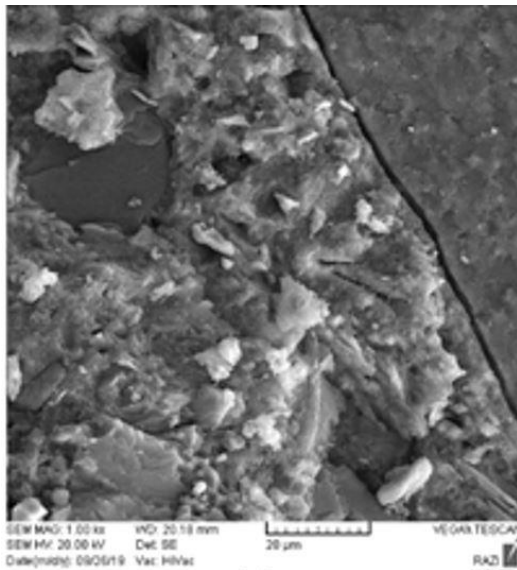
(c) OPC & MK



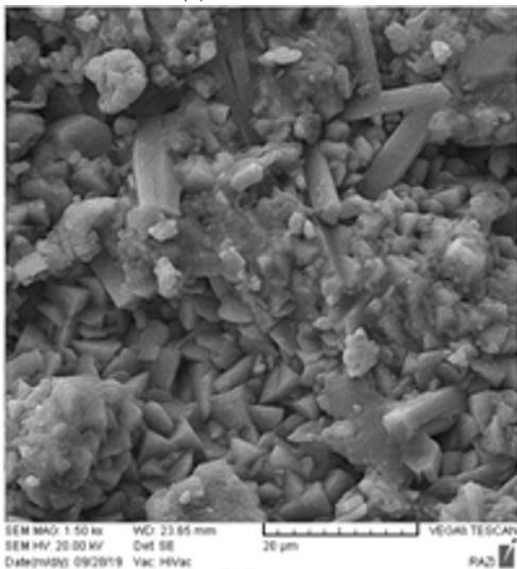
(c) OPC, MK & SF

Fig. 13 SEM images of SCC with binary mixtures

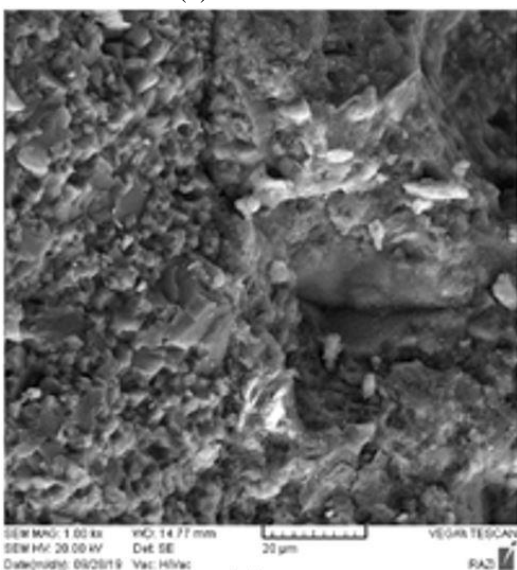
Fig. 14 SCC SEM images for ternary specimens



(a) K15 S6 F35



(b) K25 S6 F35



(c) K15 S12 F35

Fig. 15 SEM images of SCC for quaternary specimens

presence of the high C-S-H, the secondary reactions are likely to increase and the rate of strength development of these mixtures will increase dramatically with age, which is fully consistent with the results of mechanical experiments.

5. Conclusions

In this study, the rheological and mechanical properties of SCC containing three pozzolans as MK, SF, and FA with separate and simultaneous applications were investigated. On this basis, the SCC was first constructed using conventional materials along with limestone powder with an average particle size of 100 μm . In the next step, MK, SF, and FA with different percentages were replaced either as binary, ternary & quaternary mixtures to replace a part of the cement in SCC. Specimens made of SCC were tested in fresh and hardened states at different ages.

The key results of the research are as follows:

- Using of SCMs reduced the need for SP to achieve required rheology. In binary mixtures, FA, MK and SF have orderly the best performance for reducing the SP demand and in ternary and quaternary mixtures, using of SP reduced 15% and 18% respectively.

- At 7 days of age, the CS of all mixtures containing pozzolans was lower than the Ctrl, but the growth rate with the age was more significant for concrete containing pozzolans. In MK15, the CS at 180 days of age increased up to 106 MPa (18% more than Ctrl at the same age).

- In binary mixtures, MK, FA, and SF have the highest impact on the CS of SCC, respectively. In compared to 28 days of age, the maximum growth rate for MK, SF and FA were 33, 20 and 21%, respectively, while the amount for Ctrl was 19%.

- The most significant influence of using SCMs was in quaternary mixtures, which increased the 180 days of age CS up to 46% compared to 28 days of age (which is more than 2.5 times the growth rate of the Ctrl). It should be noted that for the mixture with the most rate of growth (46% for MK15SF6FA35) the replacement percentage was 56%.

- When pozzolans used separate simultaneous, analysis of CS of SCC shows the best performance as in quaternary mixtures if the growth rate is considered, and the best performance for binary mixtures if is compared to Ctrl at 28 days of age.

- The SPT at 28 days of age in all mixtures containing pozzolans was lower than the Ctrl. FA, SF, and MK have orderly the best performance in achieving SPT.

- The SME in all mixtures containing pozzolan is lower than the Ctrl. The variations in the SME of the mixtures containing pozzolans were proportional to their corresponding CS changes but had a lower increase/decrease rate.

- Using different pozzolans, the microstructure of the concrete became more amorphous and large crystals were not formed. The simultaneous application of pozzolans has resulted in greater homogeneity and improved ITZ, especially in ternary mixtures.

References

- Abedini, M. and Zhang, C. (2020), "Dynamic performance of concrete columns retrofitted with FRP using segment pressure technique", *Compos. Struct.*, **260**, 113473. <https://doi.org/10.1016/j.compstruct.2020.113473>.
- Abedini, M. and Zhang, C. (2021), "Dynamic vulnerability assessment and damage prediction of RC columns subjected to severe impulsive loading", *Struct. Eng. Mech.*, **77**(4), 441. <https://doi.org/10.12989/sem.2021.77.4.441>.
- Abedini, M., Zhang, C., Mehrmashhadi, J. and Akhlaghi, E. (2020), "Comparison of ALE, LBE and pressure time history methods to evaluate extreme loading effects in RC column", *Structures*, **28**, 456-466. <https://doi.org/10.1016/j.istruc.2020.08.084>.
- ACI 134-138 (1995), Building code requirements for structural concrete-ACI318-95, American Concrete Institute; Michigan, U.S.A.
- Afshar, A., Jahandari, S., Rasekh, H., Shariati, M., Afshar, A. and Shokrgozar, A. (2020), "Corrosion resistance evaluation of rebars with various primers and coatings in concrete modified with different additives", *Constr. Build. Mater.*, **262**, 120034. <https://doi.org/10.1016/j.conbuildmat.2020.120034>.
- AK, D., Selvi, M.T., Leela, D. and Kumar, S. (2018), "Self-compacting concrete-an analysis of properties using fly ash", *Int. J. Eng. Technol.*, **7**(2.24), 135-139. <https://doi.org/10.14419/ijet.v7i2.24.12018>.
- Alam, Z., Zhang, C. and Samali, B. (2020a), "Influence of seismic incident angle on response uncertainty and structural performance of tall asymmetric structure", *Struct. Des. Tall Spec.*, **29**(12), e1750. <https://doi.org/10.1002/tal.1750>.
- Alam, Z., Zhang, C. and Samali, B. (2020b), "The role of viscoelastic damping on retrofitting seismic performance of asymmetric reinforced concrete structures", *Earthq. Eng. Eng. Vib.*, **19**(1), 223-237. <https://doi.org/10.1007/s11803-020-0558-x>.
- Alam, Z., Sun, L., Zhang, C., Su, Z. and Samali, B. (2020c), "Experimental and numerical investigation on the complex behaviour of the localised seismic response in a multi-storey plan-asymmetric structure", *Struct. Infrastruct. E.*, **17**(1), 86-102. <https://doi.org/10.1080/15732479.2020.1730914>.
- Ardalan, R.B., Joshaghani, A. and Hooton, R.D. (2017), "Workability retention and compressive strength of self-compacting concrete incorporating pumice powder and silica fume", *Constr. Build. Mater.*, **134**, 116-122. <https://doi.org/10.1016/j.conbuildmat.2016.12.090>.
- Badogiannis, E. and Tsvivilis, S. (2009), "Exploitation of poor Greek kaolins: Durability of metakaolin concrete", *Cement Concrete Comp.*, **31**(2), 128-133. <https://doi.org/10.1016/j.cemconcomp.2008.11.001>.
- Badogiannis, E.G., Sfikas, I.P., Voukia, D.V., Trezos, K.G. and Tsvivilis, S.G. (2015), "Durability of metakaolin self-compacting concrete", *Constr. Build. Mater.*, **82**, 133-141. <http://doi.org/10.1016/j.conbuildmat.2015.02.023>.
- Badry, F. (2015), Experimental and numerical studies in self-compacting concrete, Ph.D. Dissertation, Cardiff University, Cardiff, U.K.
- Cassagnabère, F., Mouret, M., Escadeillas, G., Broilliard, P. and Bertrand, A. (2010), "Metakaolin, a solution for the precast industry to limit the clinker content in concrete: Mechanical aspects", *Constr. Build. Mater.*, **24**(7), 1109-1118. <https://doi.org/10.1016/j.conbuildmat.2009.12.032>.
- Golafshani, E.M. and Ashour, A. (2016), "Prediction of self-compacting concrete elastic modulus using two symbolic regression techniques", *Automat. Constr.* **64**: 7-19. <http://dx.doi.org/10.1016/j.autcon.2015.12.026>.
- Golewski, G. and Sadowski, T. (2014), "An analysis of shear fracture toughness KIIC and microstructure in concretes containing fly-ash", *Constr. Build. Mater.*, **51**, 207-214. <https://doi.org/10.1016/j.conbuildmat.2013.10.044>.
- Golewski, G. and Sadowski, T. (2017), "The fracture toughness the KIIC of concretes with F fly ash (FA) additive", *Constr. Build. Mater.*, **143**, 444-454. <https://doi.org/10.1016/j.conbuildmat.2017.03.137>.
- Gruber, K.A., Ramlochan, T., Boddy, A., Hooton, R.D. and Thomas, M.D.A. (2001), "Increasing concrete durability with high-reactivity metakaolin", *Cement Concrete Comp.*, **23**(6), 479-484. [https://doi.org/10.1016/S0958-9465\(00\)00097-4](https://doi.org/10.1016/S0958-9465(00)00097-4).
- Güneyisi, E., Gesoğlu, M. and Mermerdaş, K. (2008), "Improving strength, drying shrinkage, and pore structure of concrete using metakaolin", *Mater. Struct.*, **41**(5), 937-949. <https://doi.org/10.1617/s11527-007-9296-z>.
- Guo, Z., Jiang, T., Zhang, J., Kong, X., Chen, C. and Lehman, D. E. (2020), "Mechanical and durability properties of sustainable self-compacting concrete with recycled concrete aggregate and fly ash, slag and silica fume", *Constr. Build. Mater.*, **231**, 117115. <https://doi.org/10.1016/j.conbuildmat.2019.117115>.
- Hassan, A., Lachemi, M. and Hossain, K. (2010), *Effect of Metakaolin on the Rheology of Self-Consolidating Concrete*, in *Design, Production and Placement of Self-Consolidating Concrete*, Springer, Dordrecht, Netherlands.
- Iris, G.T., Belen, G.F. Jua, P. and Javier, E.L. (2017), "Prediction of self-compacting recycled concrete mechanical properties using vibrated recycled concrete experience", *Constr. Build. Mater.*, **131**, 641-654. <https://doi.org/10.1016/j.jclepro.2020.121362>.
- Jalal, M., Pouladkhan, A., Harandi, O.F. and Jafari, D. (2015), "Comparative study on effects of Class F fly ash, nano silica and silica fume on properties of high performance self-compacting concrete", *Constr. Build. Mater.*, **94**, 90-104. <https://doi.org/10.1016/j.conbuildmat.2015.07.001>.
- Khodabakhshian, A., Ghalehnovi, M. De Brito, J. and Shamsabadi, E.A. (2018), "Durability performance of structural concrete containing silica fume and marble industry waste powder", *J. Clean. Prod.*, **170**, 42-60. <https://doi.org/10.1016/j.jclepro.2017.09.116>.
- Li, D., Togholi, A., Shariati, M., Sajedi, F., Bui, D.T., Kianmehr, P., Mohamad, E.T. and Khorami, M. (2019), "Application of polymer, silica-fume and crushed rubber in the production of pervious concrete", *Smart Struct. Syst.*, **23**(2), 207-214. <https://doi.org/10.12989/sss.2019.23.2.207>.
- Liu, J., Liu, Y. and Wang, X. (2020a), "An environmental assessment model of construction and demolition waste based on system dynamics: A case study in Guangzhou", *Environ. Sci. Pollut. R.* **27**(30), 37237-37259. <https://doi.org/10.1007/s11356-019-07107-5>.
- Liu, J., Liu, Y. and Wang, X. (2020b), "Exploring factors influencing construction waste reduction: A structural equation modeling approach", *J. Clean. Prod.*, **276**, 123185. <https://doi.org/10.1016/j.jclepro.2020.123185>.
- Madandoust, R., Ranjbar, M. and Mohseni, E. (2012), "Effect of nano materials on engineering properties of self-compacting mortar containing fly ash", *Concrete Res.*, **5**(2), 55-67. <https://doi.org/10.1016/j.conbuildmat.2015.07.063>.
- Marsh, B.K. and Day, R.L. (1988), "Pozzolanic and cementitious reactions of fly ash in blended cement pastes", *Cement Concrete Res.*, **18**(2), 301-310. [https://doi.org/10.1016/0008-8846\(88\)90014-2](https://doi.org/10.1016/0008-8846(88)90014-2).
- Mehrabi, P., Shariati, M., Kabirifar, K., Jarrah, M., Rasekh, H., Trung, N.T., Shariati, A. and Jahandari, S. (2021), "Effect of pumice powder and nano-clay on the strength and permeability of fiber-reinforced pervious concrete incorporating recycled concrete aggregate", *Constr. Build. Mater.*, **287**, 122652. <https://doi.org/10.1016/j.conbuildmat.2021.122652>.

- Memon, N.A., Memon, M.A., Lakho, N.A., Memon, F.A., Keerio, M.A. and Memon, A.N. (2018), "A review on self-compacting concrete with cementitious materials and fibers", *Eng. Technol. Appl. Sci. Res.*, **8**(3), 2969-2974. <https://doi.org/10.48084/etasr.2006>.
- Memon, M.A., Memon, N.A., Memon, A.H., Bhanbhro, R. and Lashari, M.H. (2020), "Flow assessment of self-compacted concrete incorporating fly ash", *Eng. Technol. Appl. Sci. Res.*, **10**(2), 5392-5395. <https://doi.org/10.48084/etasr.3283>.
- Nosrati, A., Zandi, Y., Shariati, M., Khademi, K., Aliabad, M. D., Marto, A., Mu'azu, M., Ghanbari, E., Mandizadeh, M.B. and Shariati, A. (2018), "Portland cement structure and its major oxides and fineness", *Smart Struct. Syst.*, **22**(4), 425-432. <https://doi.org/10.12989/sss.2018.22.4.425>.
- Poon, C.S., Azhar, S., Anson, M. and Wong, Y.L. (2003), "Performance of metakaolin concrete at elevated temperatures", *Cement Concrete Compos.*, **25**(1), 83-89. [https://doi.org/10.1016/S0958-9465\(01\)00061-0](https://doi.org/10.1016/S0958-9465(01)00061-0).
- Rajaei, S., Shoaie, P., Shariati, M., Ameri, F., Musaei, H.R., Behforouz, B. and de Brito, J. (2021), "Rubberized alkali-activated slag mortar reinforced with polypropylene fibres for application in lightweight thermal insulating materials", *Constr. Build. Mater.*, **270**, 121430. <https://doi.org/10.1016/j.conbuildmat.2020.121430>.
- Sfikas, I.P., Badogiannis, E.G. and Trezos, K.G. (2014), "Rheology and mechanical characteristics of self-compacting concrete mixtures containing metakaolin", *Constr. Build. Mater.*, **64**, 121-129. <https://doi.org/10.1016/j.conbuildmat.2014.04.048>.
- Shariati, M., Heyrati, A., Zandi, Y., Laka, H., Toghroli, A., Kianmehr, P., Safa, M., Salih, M.N. and Poi-Ngian, S. (2019a), "Application of waste tire rubber aggregate in porous concrete", *Smart Struct. Syst.*, **24**(4), 553-566. <http://doi.org/10.12989/sss.2019.24.4.553>.
- Shariati, M., Rafie, S., Zandi, Y., Fooladvand, R., Gharehaghaj, B., Mehrabi, P., Shariat, A., Trung, N.T., Salih, M.N. and Poi-Ngian, S. (2019b), "Experimental investigation on the effect of cementitious materials on fresh and mechanical properties of self-consolidating concrete", *Adv. Concrete Constr.*, **8**(3), 225-237. <http://doi.org/10.12989/acc.2019.8.3.225>.
- Shariati, M., Shariati, A., Trung, N.T., Shoaie, P., Ameri, F., Bahrami, N. and Zamanabadi, S.N. (2020a), "Alkali-activated slag (AAS) paste: Correlation between durability and microstructural characteristics", *Constr. Build. Mater.*, **267**, 120886. <https://doi.org/10.1016/j.conbuildmat.2020.120886>.
- Shariati, M., Mafipour, M.S., Ghahremani, B., Azarhomayun, F., Ahmadi, M., Trung, N.T. and Shariati, A. (2020b), "A novel hybrid extreme learning machine-grey wolf optimizer (ELM-GWO) model to predict compressive strength of concrete with partial replacements for cement", *Eng. Comput.*, 1-23. <https://doi.org/10.1007/s00366-020-01081-0>.
- Shariati, M., Mafipour, M.S., Haido, J.H., Yousif, S.T., Toghroli, A., Trung, N.T. and Shariati, A. (2020c), "Identification of the most influencing parameters on the properties of corroded concrete beams using an Adaptive Neuro-Fuzzy Inference System (ANFIS)", *Steel Compos. Struct.*, **34**(1), 155. <http://doi.org/10.12989/scs.2020.34.1.155>.
- Shariati, M., Mafipour, M.S., Mehrabi, P., Ahmadi, M., Wakil, K., Trung, N.T. and Toghroli, A. (2020d), "Prediction of concrete strength in presence of furnace slag and fly ash using Hybrid ANN-GA (Artificial Neural Network-Genetic Algorithm)", *Smart Struct. Syst.*, **25**(2), 183-195. <http://doi.org/10.12989/sss.2020.25.2.183>.
- Siddique, R. and Khan, M.I. (2011), *Supplementary Cementing Materials*, Springer Science & Business Media, Berlin, Germany
- Sun, L., Li, C., Zhang, C., Su, Z. and Chen, C. (2018), "Early monitoring of rebar corrosion evolution based on FBG sensor", *Int. J. Struct. Stabil. Dyn.*, **18**(8), 1840001. <https://doi.org/10.1142/S0219455418400011>.
- Sun, L., Li, C., Zhang, C., Liang, T. and Zhao, Z. (2019), "The strain transfer mechanism of fiber bragg grating sensor for extra-large strain monitoring", *Sensors*, **19**(8), 1851. <https://doi.org/10.3390/s19081851>.
- Sun, L., Yang, Z., Jin, Q. and Yan, W. (2020), "Effect of axial compression ratio on seismic behavior of GFRP reinforced concrete columns", *Int. J. Struct. Stabil. Dyn.*, **20**(6), 2040004. <https://doi.org/10.1142/S0219455420400040>.
- Toghroli, A., Shariati, M., Karim, M.R. and Ibrahim, Z. (2017), "Investigation on composite polymer and silica fume-rubber aggregate pervious concrete", *Proceedings of the 5th International Conference on Advances in Civil, Structural and Mechanical Engineering*, Zurich, Switzerland.
- Toghroli, A., Shariati, M., Sajedi, F., Ibrahim, Z., Koting, S., Mohamad, E.T. and Khorami, M. (2018), "A review on pavement porous concrete using recycled waste materials", *Smart Struct. Syst.*, **22**(4), 433-440. <https://doi.org/10.12989/sss.2018.22.4.433>.
- Toghroli, A., Mehrabi, P., Shariati, M., Trung, N.T., Jahandari, S. and Rasekh, H. (2020), "Evaluating the use of recycled concrete aggregate and pozzolanic additives in fiber-reinforced pervious concrete with industrial and recycled fibers", *Constr. Build. Mater.*, **252**, 118997. <https://doi.org/10.1016/j.conbuildmat.2020.118997>.
- Trung, N.T., Alemi, N., Haido, J.H., Shariati, M., Baradaran, S. and Yousif, S.T. (2019), "Reduction of cement consumption by producing smart green concretes with natural zeolites", *Smart Struct. Syst.*, **24**(3), 415-425. <https://doi.org/10.12989/sss.2019.24.3.415>.
- Vejmelková, E., Keppert, M., Grzeszczyk, S., Skaliński, B. and Černý, R. (2011), "Properties of self-compacting concrete mixtures containing metakaolin and blast furnace slag", *Constr. Build. Mater.*, **25**(3), 1325-1331. <https://doi.org/10.1016/j.conbuildmat.2010.09.012>.
- Wang, N., Sun, X., Zhao, Q., Yang, Y. and Wang, P. (2020), "Leachability and adverse effects of coal fly ash: A review", *J. Hazard. Mater.*, **396**, 122725. <https://doi.org/10.1016/j.jhazmat.2020.122725>.
- Wang, N., Sun, X., Zhao, Q. and Wang, P. (2021), "Treatment of polymer-flooding wastewater by a modified coal fly ash-catalysed Fenton-like process with microwave pre-enhancement: System parameters, kinetics, and proposed mechanism", *Chem. Eng. J.*, **406**, 126734. <https://doi.org/10.1016/j.cej.2020.126734>.
- Xu, D.S., Huang, M. and Zhou, Y. (2020a), "One-dimensional compression behavior of calcareous sand and marine clay mixtures", *Int. J. Geomech.*, **20**(9), 04020137. [https://doi.org/10.1061/\(ASCE\)GM.1943-5622.0001763](https://doi.org/10.1061/(ASCE)GM.1943-5622.0001763).
- Xu, D., Liu, Q., Qin, Y. and Chen, B. (2020b), "Analytical approach for crack identification of glass fiber reinforced polymer-sea sand concrete composite structures based on strain dissipations", *Struct. Health Monit.*, 1475921720974290. <https://doi.org/10.1177/1475921720974290>.
- Xu, J., Li, Y., Ren, C., Wang, S., Vanapalli, S.K. and Chen, G. (2021), "Influence of freeze-thaw cycles on microstructure and hydraulic conductivity of saline intact loess", *Cold Reg. Sci. Technol.*, **181**, 103183. <https://doi.org/10.1016/j.coldregions.2020.103183>.
- Yang, Y., Yao, J., Wang, C., Gao, Y., Zhang, Q., An, S. and Song, W. (2015), "New pore space characterization method of shale matrix formation by considering organic and inorganic pores", *J. Natl Gas Sci. Eng.*, **27**, 496-503. <https://doi.org/10.1016/j.jngse.2015.08.017>.

- Yang, Y., Li, Y., Yao, J., Iglauer, S., Luquot, L., Zhang, K., Sun, H., Zhang, L., Song, W. and Wang, Z. (2020), "Dynamic pore-scale dissolution by CO₂-saturated brine in carbonates: Impact of homogeneous versus fractured versus vuggy pore structure", *Water Resour. Res.*, **56**(4), e2019WR026112. <https://doi.org/10.1029/2019WR026112>.
- Yazdani, M., Kabirifar, K., Frimpong, B.E., Shariati, M., Mirmozaffari, M. and Boskabadi, A. (2020), "Improving construction and demolition waste collection service in an urban area using a simheuristic approach: A case study in Sydney, Australia", *J. Clean. Prod.*, **280**, 124138. <https://doi.org/10.1016/j.jclepro.2020.124138>.
- Zhang, C.W., Ou, J.P. and Zhang, J.Q. (2006), "Parameter optimization and analysis of a vehicle suspension system controlled by magnetorheological fluid dampers", *Struct. Control Health Monit.*, **13**(5), 885-896. <https://doi.org/10.1002/stc.63>.
- Zhang, C. and Ou, J. (2008), "Control structure interaction of electromagnetic mass damper system for structural vibration control", *J. Eng. Mech.*, **134**(5), 428-437. [https://doi.org/10.1061/\(ASCE\)0733-9399\(2008\)134:5\(428\)](https://doi.org/10.1061/(ASCE)0733-9399(2008)134:5(428)).
- Zhang, C. and Wang, H. (2019a), "Swing vibration control of suspended structure using active rotary inertia driver system: Parametric analysis and experimental verification", *Appl. Sci.*, **9**(15), 3144. <https://doi.org/10.3390/app9153144>.
- Zhang, C. and Wang, H. (2019b), "Robustness of the active rotary inertia driver system for structural swing vibration control subjected to multi-type hazard excitations", *Appl. Sci.*, **9**(20), 4391. <https://doi.org/10.3390/app9204391>.
- Zhang, C., Alam, Z., Sun, L., Su, Z. and Samali, B. (2019a), "Fibre Bragg grating sensor-based damage response monitoring of an asymmetric reinforced concrete shear wall structure subjected to progressive seismic loads", *Struct. Control Health Monit.*, **26**(3), e2307. <https://doi.org/10.1002/stc.2307>.
- Zhang, H., Sun, M., Song, L., Guo, J. and Zhang, L. (2019b), "Fate of NaClO and membrane foulants during in-situ cleaning of membrane bioreactors: Combined effect on thermodynamic properties of sludge", *Biochem. Eng. J.*, **147**, 146-152. <https://doi.org/10.1016/j.bej.2019.04.016>.
- Zhang, L., Zheng, J., Tian, S., Zhang, H., Guan, X., Zhu, S., Zhang, X., Bai, Y., Xu, P. and Zhang, J. (2020a), "Effects of Al³⁺ on the microstructure and bioflocculation of anoxic sludge", *J. Environ. Sci.*, **91**, 212-221. <https://doi.org/10.1016/j.jes.2020.02.010>.
- Zhang, C., Gholipour, G. and Mousavi, A.A. (2020b), "State-of-the-art review on responses of RC structures subjected to lateral impact loads", *Arch. Comput. Method. E.*, **28**(4), 2477-2507. <https://doi.org/10.1007/s11831-020-09467-5>.
- Zhang, M., Zhang, L., Tian, S., Zhang, X., Guo, J., Guan, X. and Xu, P. (2020c), "Effects of graphite particles/Fe³⁺ on the properties of anoxic activated sludge", *Chemosphere*, **253**, 126638. <https://doi.org/10.1016/j.chemosphere.2020.126638>.
- Zhang, L., Zhang, M., You, S., Ma, D., Zhao, J. and Chen, Z. (2021), "Effect of Fe³⁺ on the sludge properties and microbial community structure in a lab-scale A²O process", *Sci. Total Environ.*, **780**, 146505. <https://doi.org/10.1016/j.scitotenv.2021.146505>.
- Zhao, X., Gu, B., Gao, F. and Chen, S. (2020), "Matching model of energy supply and demand of the integrated energy system in coastal areas", *J. Coastal Res.*, **103**(SI), 983-989. <https://doi.org/10.2112/SI103-205.1>.
- Zheng, J., Zhang, C. and Li, A. (2020), "Experimental investigation on the mechanical properties of curved metallic plate dampers", *Appl. Sci.*, **10**(1), 269. <https://doi.org/10.3390/app10010269>.
- Zhu, L., Zhang, C., Guan, X., Uy, B., Sun, L. and Wang, B. (2018), "The multi-axial strength performance of composited structural BCW members subjected to shear forces", *Steel Compos. Struct.*, **27**(1), 75-87. <http://doi.org/10.12989/scs.2018.27.1.075>.
- Ziaei-Nia, A., Shariati, M. and Salehabadi, E. (2018), "Dynamic mix design optimization of high-performance concrete", *Steel Compos. Struct.*, **29**(1), 67-75. <http://doi.org/10.12989/scs.2018.29.1.067>.
- Zuo, C., Chen, Q., Tian, L., Waller, L. and Asundi, A. (2015), "Transport of intensity phase retrieval and computational imaging for partially coherent fields: The phase space perspective", *Opt. Laser Eng.*, **71**, 20-32. <https://doi.org/10.1016/j.optlaseng.2015.03.006>.
- Zuo, C., Sun, J., Li, J., Zhang, J., Asundi, A. and Chen, Q. (2017), "High-resolution transport-of-intensity quantitative phase microscopy with annular illumination", *Scientific Reports*, **7**(1), 1-22. <https://doi.org/10.1038/s41598-017-06837-1>.
- Zuo, X., Dong, M., Gao, F. and Tian, S. (2020), "The modeling of the electric heating and cooling system of the integrated energy system in the coastal area", *J. Coastal Res.*, **103**(SI), 1022-1029. <https://doi.org/10.2112/SI103-213.1>.

AT